Journal of Mathematical Chemistry 4(1990)127-142

A THEORETICAL STUDY OF π-HYDROCARBON–IRON TRICARBONYL COMPLEXES

Jerry Ray DIAS
Department of Chemistry, University of Missouri, Kansas City, MO 64110, USA

Abstract

The molecular orbital parameters for tricarbonyl(tetrahapto-unsaturated-hydrocarbon)iron complexes are computed using graph-theoretical methods. The results are in agreement with their experimental properties.

1. Introduction

Merging the graph-theoretical methods previously developed by the author [1–8] with the topological Hückel model developed by Mingos [9], one can rapidly compute the characteristic polynomials and eigenvalues of olefin–metal complexes. This leads to a facile noncomputer oriented method for obtaining useful Hückel MO parameters. The ease with which these calculations are performed not only facilitates our chemical thinking processes, but also provides us with a unique perspective in the conceptualization of chemical phenomena. The study of different ways of comparing molecules contributes to our better understanding of their chemistry. Herein, we present a study of carbonylmetal η^4-olefin complexes using these methods. A structure-resonance theory study of these metal complexes has been reported [10].

The Mingos model assumes the basis-set orbitals for the π-electron calculation as being the hydrocarbon polyene $p\pi$ orbitals (i.e. unhybridized carbon p_z orbitals) and each of the metal e_{xz} ($d_{xz} + p_x = 2e_{xz}$) and e_{yz} ($d_{yz} + p_y = 2e_{yz}$) hybrid orbitals (fig. 1). The metal and carbon Coulomb integrals ($\alpha_c = \alpha_m = \alpha$) and carbon–carbon $2p\pi$–$2p\pi$ and the metal–carbon e_{xz}–$2p\pi$ and e_{yz}–$2p\pi$ exchange integrals ($\beta_{cc} = \beta_{cm} = \beta$) are taken to be comparable; the effect of electronegativity differences on α_m can be introduced as an additional refinement later on. The signs of the metal–carbon exchange integrals (β) are chosen to reflect the phase changes in the chosen set of basis orbitals: $-\beta$ is associated with a phase change (fig. 1); a single phase change in a cyclic π-network is a Möbius system [11]. A double phase change acts like a double negative to give a "normal cycle".

These assumptions describe the metal–polyene fragment as being perturbed to a negligible extent by the carbonyl groups. Justification for this derives from both experimental and theoretical studies [12,13]. The basis orbitals for tricarbonyl(η^4-butadiene)iron and tricarbonyl(η^4-cyclobutadiene)iron with their corresponding molecular graphs are depicted in fig. 1. The iron d_{xz}–p_x and d_{yz}–p_y hybrid

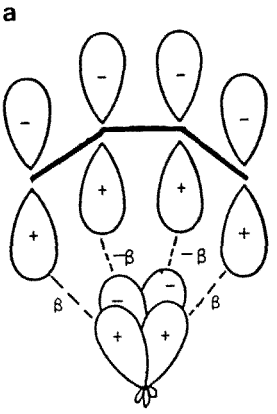

(a) Basis orbitals for $Fe(\eta^4\text{-}C_4H_6)(CO)_3$

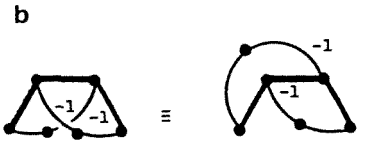

(b) Orbital network graph for $Fe(\eta^4\text{-}C_4H_6)(CO)_3$

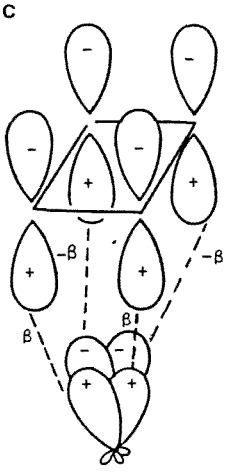

(c) Basis orbitals for $Fe(\eta^4\text{-}C_4H_4)(CO)_3$

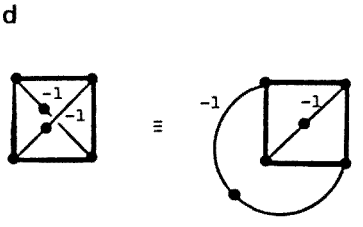

(d) Orbital network graph for $Fe(\eta^4\text{-}C_4H_4)(CO)_3$

Fig. 1. Basis orbitals and corresponding orbital network graphs for $Fe(\eta^4$-unsaturated-hydrocarbon$)(CO)_3$ complexes.

orbitals combine with the organic ligand p_z orbitals to form a three-dimensional delocalized electronic network containing N_c electrons, where N_c is the total number of basis orbitals. The $Fe(CO)_3$ moiety is characterized by the electronic configuration $(e_{xz})^1(e_{yz})^1$, with its remaining six metal electrons occupying the non-bonding d_{z^2}, $d_{x^2-y^2}$, and d_{xy} orbitals. Thus, the $Fe(CO)_3$ group contributes two electrons for metal–butadiene bonding.

In this work, an orbital network graph (fig. 1) is a graph where vertices correspond to atomic π-orbitals and edges (lines) connecting the vertices associate the pairs

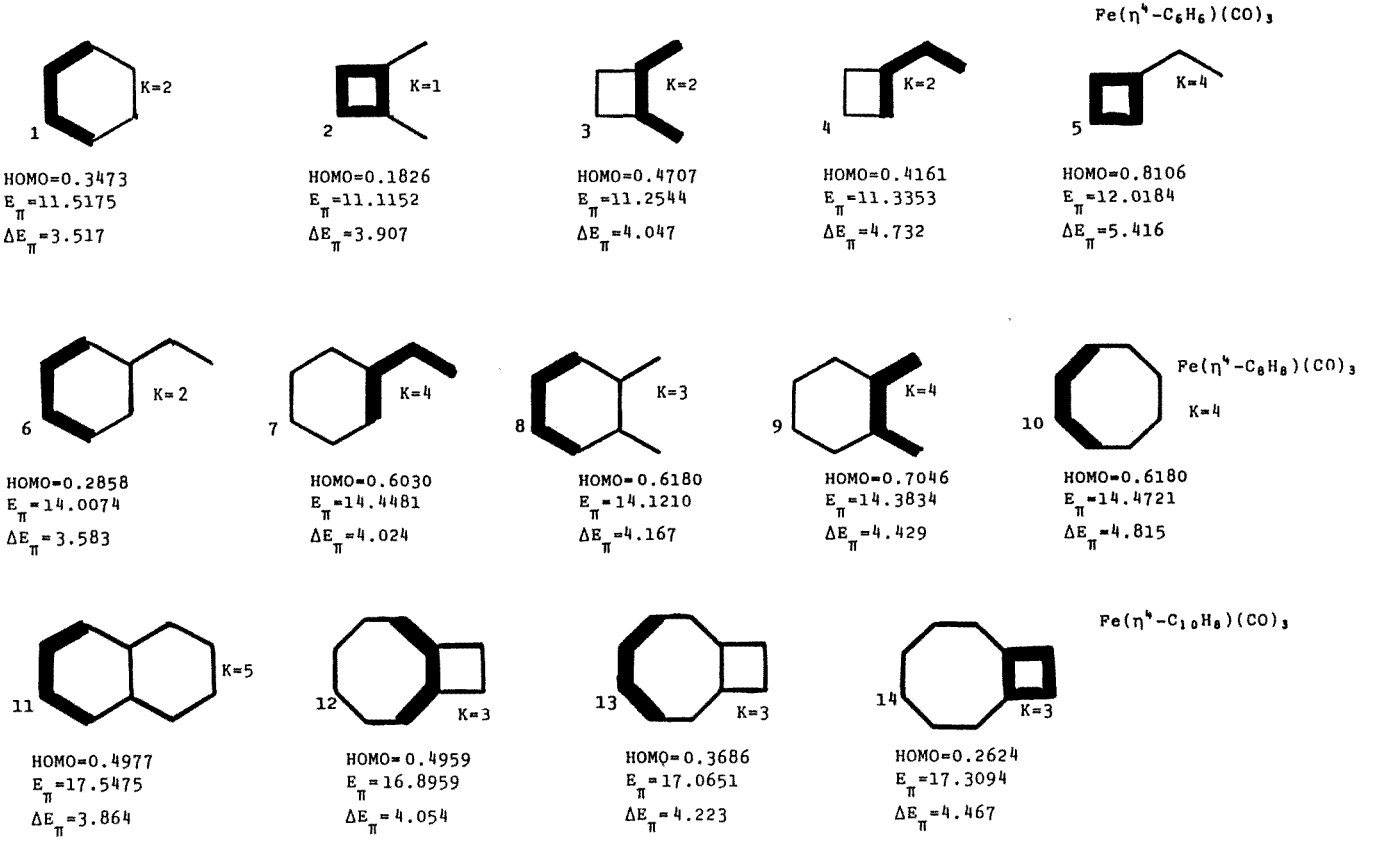

Fig. 2 (continued on following page).

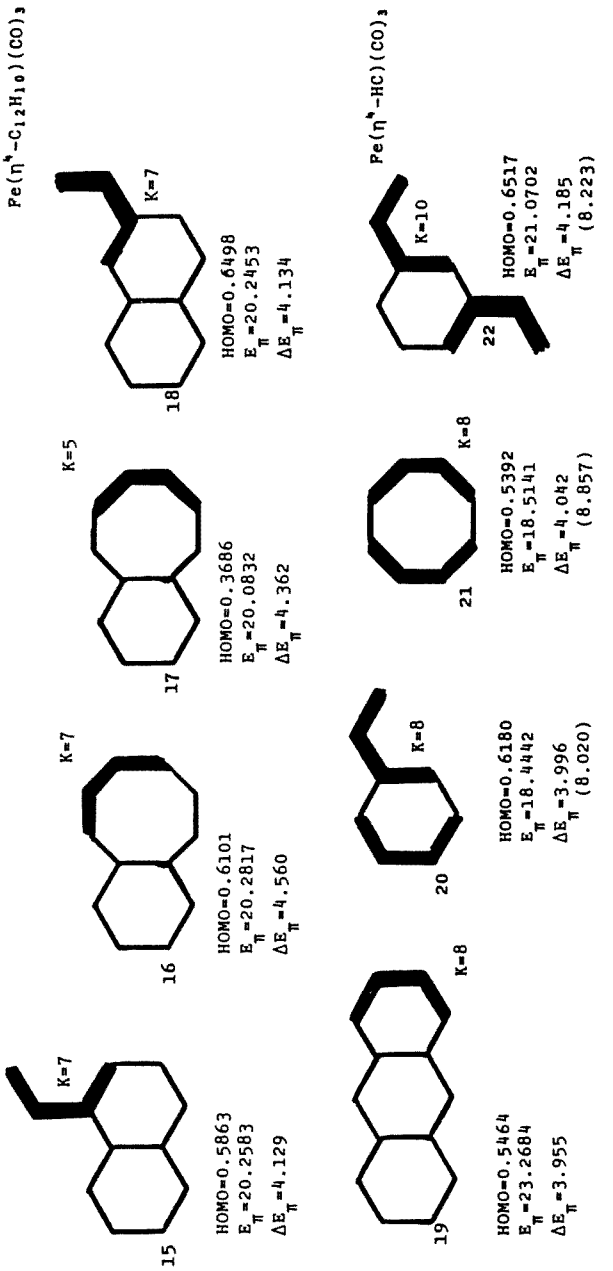

Fig. 2 (continued on following page).

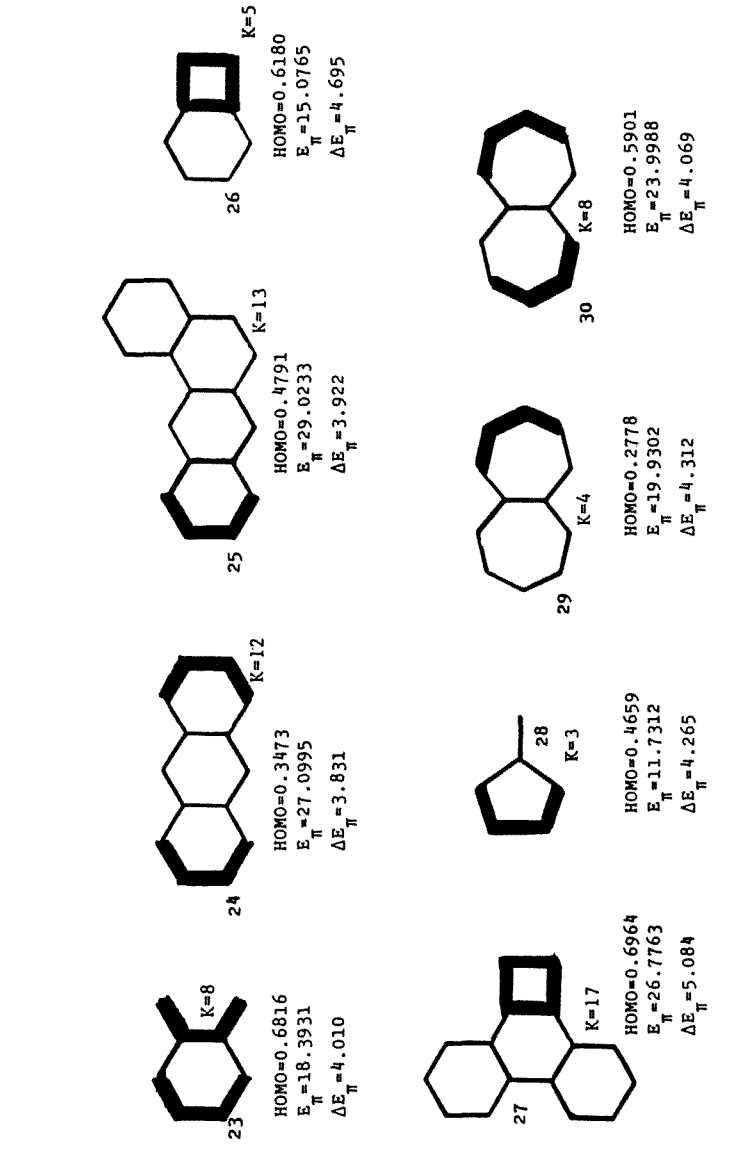

Fig. 2. HMO parameters for various Fe(η^4-unsaturated-hydrocarbon)$(CO)_3$ complexes.

of π-orbital interactions. It should be noted that orbital network graphs and their corresponding computed parameters disregard stereochemistry, and the following two orbital network graphs for $Fe(\eta^4\text{-}C_4H_6)(CO)_3$ give identical characteristic polynomials.

Thus, the computed Hückel MO parameters presented herein disregard the molecular folding found in **10** and **21** (fig. 2) and the existence of *cis* and *trans* isomers found in **20** to **24** and **30**, and the metal basis orbitals can be rotated to give two different but energetically equivalent alignments with regard to the butadiene basis orbitals. In fig. 2, the site of the tricarbonyliron attachment is indicated by heavy lines.

2. Determining characteristic polynomials and eigenvalues with graph theory

Making use of graph-theoretical methods previously published, one can quickly determine the characteristic polynomials and eigenvalues of the tricarbonyliron complexes presented in fig. 2. Table 1 gives a glossary of terms and table 2 gives a summary of the equations that will be used. The tetrahapto–iron complexes of butadiene and cyclobutadiene and compounds **1** to **27** shown in fig. 2 are alternant π-electronic networks (i.e. contain no odd-sized rings) with bonding/antibonding MO energy levels that are paired and that have characteristic polynomials with only even terms and a tail coefficient which equals the corrected structure count (CSC = K) to the second power. Herndon's method for determining CSC can be used to obtain the tail coefficient $a_N = \pm K^2$ of the characteristic polynomial of alternant π-electronic networks [10]. The second coefficient $a_2 = -q$ is equal to the negative of the number of σ-bonds in the orbital network graph of the metal carbonyl complex molecule. The a_4 and a_6 coefficients are given by eq. (1) and eq. (2), respectively, in table 2. In the application of these latter two, it should be noted that r_4 and r_6 give the algebraic sum of the number of tetragonal and hexagonal rings, respectively, where Möbius ring systems are assigned negative values. Also, r_4 and r_6 represent all combinatorial tetragonal and hexagonal circuits, respectively. For example, the octahedron possesses fifteen different tetragonal circuits (each of the twelve octahedron edges is central to one tetragonal circuit and each of the three pairs of opposing vertices is central to a tetragonal circuit), and the cube has sixteen distinct hexagonal circuits (each of the twelve cube edges is central to one hexagonal circuit and each of the four pairs of opposing vertices is central to a hexagonal circuit). It should be noted that eq. (1) and eq. (3) are valid for all graphs, and eq. (2) is valid for all graphs having vertices of degree 3 or less; all the equations in table 2 were derived by the author, although some have less general precursors that were previously presented in the literature [1–8].

Table 1

Glossary of terms

a_4	– fourth coefficient in the characteristic polynomial
a_6	– sixth coefficient in the characteristic polynomial
α (α_c)	– HMO Coulomb integral (of carbon)
α_3	– number of branches on a trigonal ring
α_4	– number of branches on a tetragonal ring
β	– HMO exchange integral
C_n	– cycle or circuit of size n
d_i	– number of vertices of degree i
$e(i,j)$	– number of edges with a vertex of degree i at one end and a vertex of degree j at the other end
e_k	– an edge of weight k
ε	– energy level or HMO eigenvalue
E_π	– total pπ energy
G	– a molecular or isoconjugate graph
G_x	– a molecular graph with a single weighted vertex
G_k	– a molecular graph with a single weighted edge
h	– the weight of a heteroatom vertex [$h = (\alpha_x - \alpha_c)/\beta$]
k	– the weight of an edge [$k = \beta_{cx}/\beta_{cc}$]
L_n	– linear polyconjugated system of size n
N (N_c)	– number of (carbon atom) vertices
$P(G;X)$	– characteristic polynomial of a molecular graph
q	– number of C–C σ-bond edges
r_n	– number of rings (cycles) of n vertices
r'_3	– number of combinatorial pairs of trigonal rings
v	– vertex
X	– $(\varepsilon - \alpha)/\beta$ = graph eigenvalue
Z_k	– cycles containing edge k

To illustrate the use of the equations in table 2 for generating the characteristic polynomials, we will now present the solutions to the graph of the cube and the orbital network graphs of tricarbonyl(η^4-cyclobutadiene)iron and tricarbonyl(η^4-benzene)iron. For the cube graph $q = 12$, $a_4 = 30$, $a_6 = -28$, and $K = 3$, which gives $P(\text{cube};X) = X^8 - 12X^6 + 30X^4 - 28X^2 + 9$ [14]. For the tricarbonyl(η^4-cyclobutadiene)iron molecular graph (fig. 1), $N_c = 6$, $q = 8$, and $e(3, 3) = 4$. Figure 3 shows all the tetragonal and hexagonal circuits for this molecular graph; there are four Möbius and one regular tetragonal circuits, and two hexagonal circuits crossing over two negative unit weighted edges giving $r_4 = -4$ with $\alpha_4 = 3$, $r_4 = 1$ with $\alpha_4 = 4$, and $r_6 = 2$. Inputting these parameters into eqs. (1), (2), and (3) gives the characteristic polynomial for tricarbonyl(η^4-

Table 2

Equations for the calculation of characteristic polynomials of molecular graphs

Eq. no.	Equation
(1)	$a_4 = (1/2)(q^2 - 9q + 6N_c) - 2r_4 - d_1 - d_4 - 3d_5 - 6d_6 - \ldots$
(2)	$a_6 = -(1/6)(q^3 - 27q^2 + 116q) - N_c(3q - 16) - 2r_6 - e(3, 3) + (q - 6)e(2, 1) + (q - 5)e(3, 1) + 2\Sigma(q - 4 - \alpha_4)r_4 + r_3 + 4r_3'$
(3)	$P(G,X) = X^N - qX^{N-2} - 2r_3X^{N-3} + a_4X^{N-4} - [2r_5 - 2(q - 3 - \alpha_3)r_3]X^{N-5} + a_6X^{N-6} + \ldots$
(4)	$P(G_x;X) = XP(G_x - v_x;X) - hP(G_x - v_x;X) - k^2[XP(G_x - v_x;X) - P(G;X)]$ for edge/vertex weighted graphs
(5)	$P(G_k;X) = P(G_k - e_k;X) - k^2P(G_k - (e_k);X) - 2k\Sigma P(G_k - Z_k;X)$ for edge weighted graphs
(6)	$P(G_0;X) = P(G;X) + P(G_0 - v_0;X)$ for right mirror-plane fragment
(7)	$P(G_{e1};X) = P(G_{e1} - e_\omega;X) - P(G_{e1} - (e_\omega);X) + \Sigma P(G_{e1} - Z_\omega;X)$ for the identical fragments of vertex-centric 3-fold graphs
(8)	$P(G_{e2};X) = P(G_{e2} - e_\omega;X) - P(G_{e2} - (e_\omega);X) - \Sigma P(G_{e2} - Z_\omega;X)$ for the identical fragments of ring-centric 3-fold graphs
(9)	$P(L_n;X) = XP(L_{n-1};X) - P(L_{n-2};X)$, where $P(L_0;X) = 1$ and $P(L_1;X) = X$

cyclobutadiene)iron as $P(\text{TCCBI};X) = X^6 - 8X^4 + 20X^2 - 16$; the tail coefficients can be verified by using Herndon's CSC method [10]. Finally, for tricarbonyl(η^4-benzene)iron (**1** in fig. 2; compare with the orbital network graph in fig. 5), $N_c = 8$, $q = 10$, and $e(3, 3) = 3$. The metal complex **1** has two Möbius tetragonal rings ($r_4 = -2$), each having three branches ($\alpha_4 = 3$) and two Möbius and two regular hexagonal circuits ($r_6 = -2 + 2 = 0$) giving $P(\mathbf{1};X) = X^8 - 10X^6 + 33X^4 - 37X^2 + 4$, where the tail coefficient was obtained from the CSC. In this way, all alternant molecular graphs up to $N_c = 6$ and all alternant molecular graphs with vertices of degree 3 or less up to $N_c = 8$ can be solved. The solution of larger molecular graphs requires knowledge of some eigenvalues via embedding or by decomposition per eq. (5) into smaller graphs.

The determination of the characteristic polynomial of a non-alternant metal complex is illustrated by **28**, which has $N_c = 8$, $q = 10$, $r_4 = -2$, $r_5 = 1 - 1 - 1 = -1$,

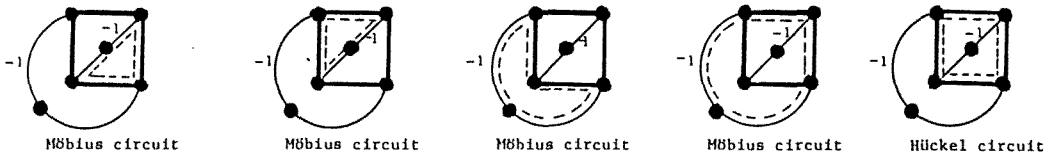

(a) All the tetragonal circuits in $Fe(\eta^4\text{-}C_4H_4)(CO)_3$ are shown by the dashed outlines.

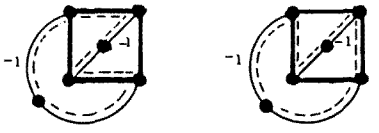

(b) All the hexagonal circuits in $Fe(\eta^4\text{-}C_4H_4)(CO)_3$ are shown by the dashed outlines.

Fig. 3. All the tetragonal and hexagonal circuits (dashed outlines) in $Fe(\eta^4\text{-}C_4H_4)(CO)_3$.

$r_6 = 1$, $r_7 = 2$, and $d_1 = 1$. Application of eqs. (1) to (3) gives $X^8 - 10X^6 + 32X^4 + 2X^3 - 36X^2 - 6X + 9$, where the tail coefficient can be obtained by the method of Herndon [10] and a_7 is the sum of $2C_7 + 2(C_5 + K_2)$ graph components with sign inversions for Möbius circuits.

Complexes **1**, **6**, **8**, **10**, **11**, **13**, **16**, **17**, **19**, **21**, **24**, **25**, **28**, **29** and **30** have no vertices larger than degree 3, and we will outline how to obtain the characteristic polynomial of some of these complexes. Application of eq. (5) decomposes **6** into fragments that are solved per eqs. (1) to (4) to give

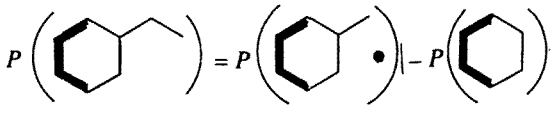

$$= X^{10} - 11X^8 + 41X^6 - 57X^4 + 19X^2 - (X^8 - 10X^6 + 33X^4 - 37X^2 + 4)$$
$$= X^{10} - 12X^8 + 51X^6 - 90X^4 + 56X^2 - 4.$$

The end terms of eq. (5) are zero when one operates on a pendant side chain, as was done for **6**. Successive decomposition of **11** per eq. (5) gives

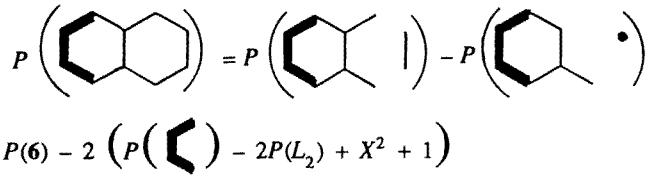

$$= (X^2-1)(X^{10}-12X^8+50X^6-84X^4+49X^2-9)-(X^{10}-11X^8+41X^6-57X^4+19X^2)$$
$$-(X^{10}-12X^8+51X^6-90X^4+56X^2-4)-2(X^6-7X^4+14X^2-6)$$
$$= X^{12}-15X^{10}+85X^8-228X^6+294X^4-161X^2+25.$$

Figure 5 summarizes the computation of the characteristic polynomial of **24**.

3. Kekulé and corrected structure count

While it is well known that the square root of the tail coefficient to the characteristic polynomial of an alternant (bipartite) molecular graph equals the difference in the number of structures of positive and negative parities (CSC), it has also been explicitly recognized that if the tail coefficient of a characteristic polynomial corresponding to a graph has an integral square root, then this value can give the difference in the number of structures of positive and negative parities, regardless of whether the graph is bipartite or not, under the following conditions. Deletion of a vertex from a non-alternant graph to give an odd alternant graph possessing a nonbonding molecular orbital (NBMO) can have the unnormalized integral coefficients of this orbital written by inspection [10,15]. The difference in the number of structures of positive and negative parities (CSC) to the non-alternant graph is given by the algebraic sum of these coefficients adjacent to the deleted vertex. The square of this number [$a_N = \pm(\mathrm{CSC})^2$] gives the tail coefficient to the characteristic polynomial of the corresponding non-alternant graph (cf. complexes **28–30**). Also, the sum of the squares of the unnormalized integral coefficients to the NBMO of an odd alternant molecular graph equals the tail coefficient to the corresponding characteristic polynomial; e.g. G_2 in fig. 4 gives 6 for the tail coefficient. For totally aromatic molecular graphs, the number of Kekulé structures equals the corrected structure count (K = CSC). Herein, we make no notational distinction between K and CSC.

Another method for determining K values of a molecular graph G uses the following relationship

$$K(G) = \pm K(G-e) \pm K(G-(e)),$$

where $G-e$ is the graph obtained upon deletion of some edge e, $G-(e)$ is the corresponding graph obtained upon deletion of edge e with its associated vertices, and the negative sign is only chosen to give a positive (or zero) $K(G)$ value when e belongs to an anti-aromatic ring [16,17]. By knowing a few K values of some small molecular

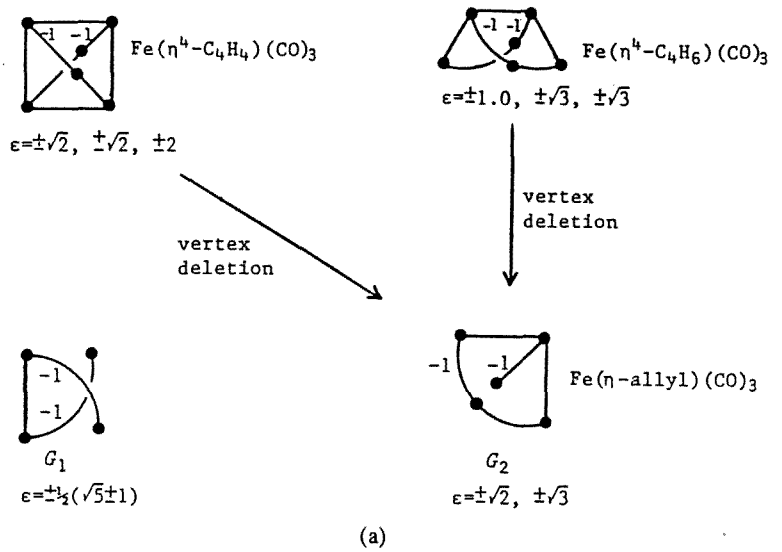

Fig. 4. Embedding fragments of Fe(η^4-unsaturated-hydrocarbon)$(CO)_3$ complexes. (a) Embedding fragments. (b) Ethene embedding on Fe(η^4-C_4H_6)$(CO)_3$.

graphs, one can use this relationship to obtain K values for larger molecular graphs. In this work, it is worthwhile to remember these values for the tricarbonyliron complexes of butadiene (K = 3), cyclobutadiene (K = 4), and benzene (K = 2). To illustrate, consider complex **11** as follows:

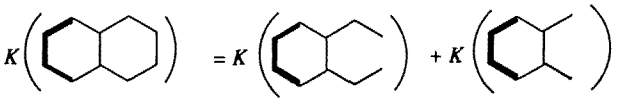

$$= K(\mathbf{11}) = K(\mathbf{1}) + K(\mathbf{8}) = 2 + 3 = 5.$$

We denote the molecular graphs of ethene (L_2), allyl (L_3), butadiene (L_4), cyclobutadiene (C_4), and benzene (C_6) by their standard graph-theoretical designations. Even carbon polyene side chains on a ring system do not change the K value of the ring, as can be noted by comparing **1** versus **6** and tricarbonyl(η^4-cyclobutadiene)iron versus **5**.

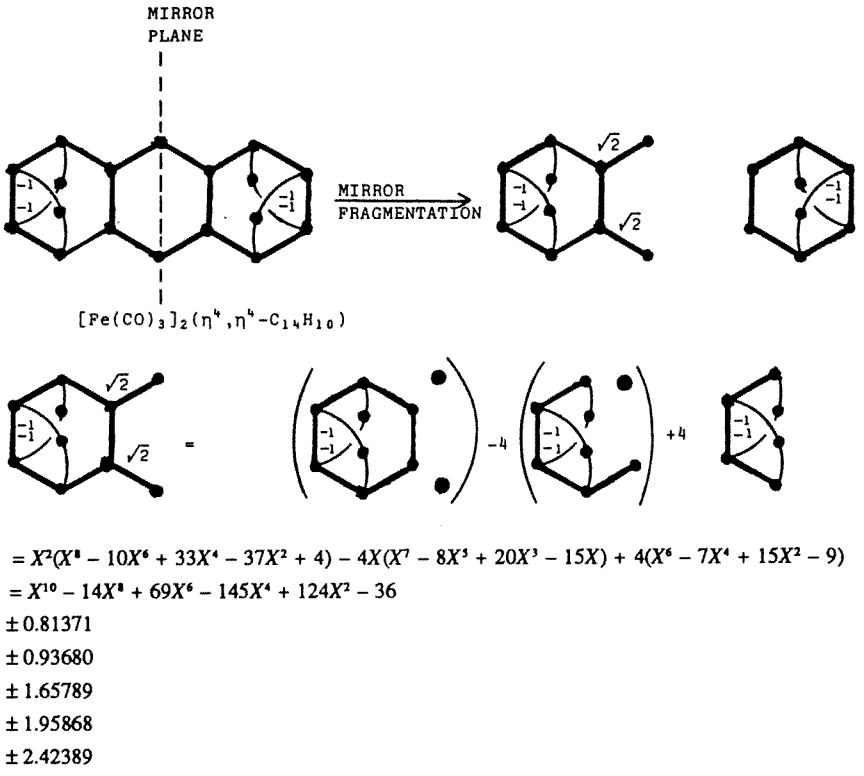

$= X^2(X^8 - 10X^6 + 33X^4 - 37X^2 + 4) - 4X(X^7 - 8X^5 + 20X^3 - 15X) + 4(X^6 - 7X^4 + 15X^2 - 9)$

$= X^{10} - 14X^8 + 69X^6 - 145X^4 + 124X^2 - 36$

± 0.81371

± 0.93680

± 1.65789

± 1.95868

± 2.42389

Fig. 5. Determination of eigenvalues by mirror plane fragmentation.

The K value of the acene complexes is given by $K(\text{acene}) = 3r_6 - 1$, as can be seen by comparing **1**, **11**, and **19**. Another representative application of this equation gives $K(\mathbf{25}) = K(\mathbf{19}) + K(\mathbf{11}) = K(\mathbf{8}) \cdot K(C_{10}H_8) + K(\mathbf{1}) \cdot K(C_6) = 13$, where the first equality was obtained by operating on edge b and the second by operating simultaneously on edges h and p of **25**. As a final example, consider **14**: $K(\mathbf{14}) = -K(\mathbf{2}) + K(\text{TCCBI}) = -1 + 4 = 3$, where the minus sign is the result of operating on the edge (e) of the anti-aromatic cyclooctatetraene ring. Note that in these examples, we avoided operating on the negative weighted edges associated with the attached tricarbonyliron moiety.

4. Eigenvalues by embedding

A molecule possessing a subset of eigenvalues found in another molecule is said to be subspectrally related to it [2,18]. If a smaller molecule can be embedded onto a larger molecule, then the eigenvalues of the smaller one will be found among the eigenvalues of the larger one [2,19]. To embed a fragment onto an alternant molecule, (a) all atoms connected directly to the fragment must be nodes (have zero coefficients in the corresponding eigenvectors), (b) on the other side of each of these nodes there will

be a repetition of the fragment with the opposite sign, and (c) other branches at these nodes will also be nodes. Common embedding fragments include ethene ($\varepsilon = \pm 1.0\beta$), allyl ($\varepsilon = \pm\sqrt{2}\beta$), 1, 3-butadiene [$\varepsilon = \pm 0.5(\sqrt{5} \pm 1)$], and pentadienyl ($\varepsilon = \pm 1.0, \pm\sqrt{3}$). Mixed embedding requires that the different fragments have some common eigenvalues, like ethene and pentadienyl ($\varepsilon = \pm 1.0$). In this work, mixed embedding with the fragments shown in fig. 4 was observed. Tricarbonyl(η^4-butadiene)iron and the metal complexes **3**, **9**, **10**, **12**, and **17** (fig. 2) all are embeddable by ethene and have, therefore, eigenvalues of $\varepsilon = \pm 1.0\beta$. Mixed embedding of butadiene and G_1 in fig. 4 occurs in the metal complexes of **8**, **10**, **19**, and **20**, which have eigenvalues of $\varepsilon = \pm 0.5(\sqrt{5} \pm 1)\beta$. For allyl, G_2, or mixed allyl and G_2 embedding to be possible, the tail coefficient or K = CSC of a test structure must be divisible by 2. Mixed allyl and G_2 embedding of **7** ($K = 4$) and G_2 embedding of **21** ($K = 2$) occurs; since there are two distinct G_2 embeddings on **21**, it is doubly degenerate in the eigenvalues of $\varepsilon = \pm\sqrt{2}\beta$. For pentadienyl, G_2, or mixed pentadienyl and G_2 embedding to occur, the test structure must have a K value divisible by 3. Two distinct mixed embeddings of pentadienyl and G_2 occur on **14** ($K = 3$), which is doubly degenerate in eigenvalues of $\varepsilon = \pm\sqrt{3}\beta$. Molecular graphs that have a doubly degenerate eigenvalue subset can have any vertex atom deleted, replaced, or augmented by a polyene substituent, giving successor molecular graphs still retaining this eigenvalue subset once. The tricarbonyliron complexes of *s-cis*-1, 3-butadiene and cyclobutadiene are doubly degenerate in eigenvalues of $\varepsilon = \pm\sqrt{3}, \pm\sqrt{3}\beta$ and $\varepsilon = \pm\sqrt{2}, \pm\sqrt{2}\beta$, respectively, and deletion of a carbon vertex from either can generate molecular graph G_2 in fig. 4, which has $\varepsilon = \pm\sqrt{2}, \pm\sqrt{3}\beta$. Attachment of a vinyl substituent to tricarbonyl(η^4-cyclobutadiene)iron gives **5**, which has $\varepsilon = \pm\sqrt{2}\beta$. Complexes **8**, **10**, **20**, and **26**, which are mixed embeddable by G_1 and L_4, all have the same HOMO = 0.6180β value, and **24** can be embedded by **1** and both have the same HOMO = 0.3473β value.

5. ΔE_π as a relative measure of reaction spontaneity

It is assumed in this work that the reaction of a polyene to form a tricarbonyliron complex will have its relative spontaneity governed principally by the change in π-electronic delocalization energy. Thus, in the following reaction scheme $\Delta E_\pi = E_\pi[\text{polyene–Fe(CO)}_3] - E_\pi[\text{polyene}]$ is a relative measure of the tendency for the reaction to take place:

$$\text{polyene} + \text{Fe(CO)}_3 \rightarrow \text{polyene–Fe(CO)}_3.$$

There are two basic kinds of (tetrahapto-polyene)metal complexes. These are typified by the known *s-cis*-1, 3-butadiene and cyclobutadiene complexes of tricarbonyliron (fig. 1). The large difference in the ΔE_π values between tricarbonyl(η^4-butadiene)iron ($\Delta E_\pi = 4.456\beta$) and tricarbonyl($\eta^4$-cyclobutadiene)iron ($\Delta E_\pi = 5.657\beta$) is consistent with the three-dimensional aromatic properties [20] exhibited by the latter metal complex [9]. The carbon–carbon bond lengths in tricarbonyl(η^4-cyclobutadiene)iron

are all equal, and this complex is known to undergo electrophilic substitution and to resist Diels–Alder reactions. Of all the $Fe(\eta^4\text{-}C_{10}H_8)(CO)_3$ isomers (fig. 2), only **14** is known, which is consistent with its larger ΔE_π value [21].

Consider the isomer group **1** to **5**. Only **3** and **5** have been synthesized [21]. The hypothetical reaction of vinylcyclobutadiene with $Fe(CO)_3$ should lead to **5** over **4** because of the larger ΔE_π for the former. Similarly, 1, 2-dimethylenylcyclobutadiene would preferentially form **3** over **2** because of its larger ΔE_π. Since the synthesis of **1** and **11** has not been accomplished, whereas **19** has been synthesized, it appears that for tetrahapto complexes of tricarbonyliron to form, ΔE_π needs to be greater than 3.9. In the isomer group of **6** to **10**, only **7**, **9**, and **10** have been prepared. Again, according to the relative ΔE_π values, $Fe(CO)_3$ should react with *ortho*-quinodimethane to preferentially form **9** over **8**. Similarly, **7** should preferentially form over **6**. In the isomer group **11** to **14**, only **13** and **14** are known to exist, which is consistent with their higher ΔE_π values. Isomers **15** to **18** are all known to exist, although **17** is only a fluxional transient species of **18**. The *bis*-tricarbonyliron complexes of **20** to **23** are known, but **24** is not known, which is consistent with its ΔE_π being below 3.9. The synthesis of tricarbonyliron complexes of **25** to **30** has been reported. Complex **25** is an example of a carcinogen, and complexes **28** to **30** are examples of non-alternant structures. Complex **27** has the second largest ΔE_π value in fig. 2 and can be regarded as the analog of triphenylene, which is the most stable $C_{18}H_{12}$ benzenoid isomer; the uncomplexed hydrocarbon corresponding to **27** is not known and is predicted to be reactive since its HOMO value is 0.0835β and its $E_\pi = 21.6928\beta$, which are smaller than those of its synthesized isomers. Similarly, **26** is the electronic analog of naphthalene, and its complexation with another tricarbonyliron leads to ferraindene coproducts that result from cyclobutadiene ring rupture.

The HOMO values for the tricarbonyliron complexes given in fig. 2 should be useful in predicting the relative ease of electrophilic and Diels–Alder reactions of their associated organic moieties. It was thought that the Diels–Alder reaction (400 °C) of **9** with methyl propynoate is preceded by dissociation to *o*-quinodimethane. However, isomerization **9** to **8** followed by Diels–Alder condensation and subsequent decomposition of the resulting tricarbonyliron complex is also plausible. In fact, this latter is even more reasonable in the light of the observation that **9** undergoes pyrolysis to benzocyclobutene of 500 °C. The more facile Friedel–Crafts acetylation of **9** over benzene is consistent with its HOMO value of 0.7046β versus 1.0β for benzene. The $Fe(CO)_3$ group in acetylergosterol complexes successfully protects the conjugated diene unit, allowing reactions of the free double bond on the 17-side chain. This result suggests that the HOMO value for the tricarbonyl(η^4-butadiene)iron unit should be equal to or greater than the HOMO value of 1.0β for ethene.

6. Summary

The diene–tricarbonyliron complexes constitute a very large class of organoiron compounds. While reviewing polycyclic member compounds of this chemical class, we

Table 3

Characteristic polynomials of π-hydrocarbon–iron–tricarbonyl complexes

Cpd	$P(G;X) - X^N + qx^{N-2}$
1	$+33X^4 - 37X^2 + 4$
2	$+31X^4 - 31X^2 + 1$
3	$+29X^4 - 24X^2 + 4$
4	$+30X^4 - 28X^2 + 4$
5	$+33X^4 - 42X^2 + 16$
6	$+51X^6 - 90X^4 + 56X^2 - 4$
7	$+51X^6 - 94X^4 + 72X^2 - 16$
8	$+50X^6 - 84X^4 + 49X^2 - 9$
9	$+50X^6 - 88X^4 + 65X^2 - 16$
10	$+52X^6 - 97X^4 + 72X^2 - 16$
11	$+85X^8 - 228X^6 + 294X^4 - 161X^2 + 25$
12	$+81X^8 - 190X^6 + 186X^4 - 72X^2 + 9$
13	$+83X^8 - 208X^6 + 231X^4 - 94X^2 + 9$
14	$+85X^8 - 229X^6 + 295X^4 - 150X^2 + 9$
15	$+113X^{10} - 379X^8 + 685X^6 - 656X^4 + 301X^2 - 49$
16	$+114X^{10} - 386X^8 + 701X^6 - 668X^4 + 301X^2 - 49$
17	$+114X^{10} - 385X^8 + 692X^6 - 639X^4 + 259X^2 - 25$
18	$+113X^{10} - 378X^8 + 679X^6 - 644X^4 + 292X^2 - 49$
19	$+162X^{12} - 687X^{10} + 1643X^8 - 2219X^6 + 1597X^4 - 532X^2 + 64$
20	$+99X^8 - 298X^6 + 447X^4 - 300X^2 + 64$
21	$+100X^8 - 308X^6 + 480X^4 - 336X^2 + 64$
22	$+129X^{10} - 474X^8 + 952X^6 - 1024X^4 + 531X^2 - 100$
23	$+98X^8 - 289X^6 + 423X^4 - 281X^2 + 64$
24	$+242X^{14} - 1334X^{12} + 4373X^{10} - 8670X^8 + 10093X^6 - 6356X^4 + 1828X^2 - 144$
25	$+264X^{16} - 1542X^{14} + 5476X^{12} - 12233X^{10} + 17184X^8 - 14736X^6 + 7232X^4 - 1797X^2 + 169$
26	$+60X^6 - 122X^4 - 104X^2 - 25$
27	$+219X^{14} - 1132X^{12} + 3491X^{10} - 6635X^8 + 7734X^6 - 5307X^4 + 1942X^2 - 289$
28	$+32X^4 + 2X^3 - 36X^2 - 6X + 9$
29	$+114X^{10} - 384X^8 + 680X^6 + 2X^5 - 596X^4 - 10X^3 + 209X^2 + 12X - 16$
30	$+182X^{12} - 842X^{10} + 4X^9 + 223X^8 - 44X^7 - 3414X^6 + 176X^5 + 2777X^4 - 300X^3 - 981X^2 + 180X + 64$

have shown how to rapidly determine their Hückel molecular parameters using chemical graph theory without the aid of a computer or group theory. This work contributes further toward the comprehensive application of graph theory in the determination of the characteristic polynomials and eigenvalues of molecules.

It has been shown that a difference in the electronic pπ energy of the complex and reactant polyene (ΔE_π) reliably predicts the chemistry of diene–tricarbonyliron complexes. These results are in complete agreement with localization energy calcu-

lations [22] associated with the polyene reactant and with structure-resonance theory calculations associated with the complex [10]. The critical value of ΔE_π below which synthesis of a diene–tricarbonyliron complex appears to be difficult is $\sim 3.9\beta$.

References

[1] J.R. Dias, Theor. Chim. Acta 68(1985)107–123; 77(1989), in press.
[2] J.R. Dias, J. Mol. Struct. (THEOCHEM) 149(1987)213–241; 165(1988)125–148; 185(1989)57–81.
[3] J.R. Dias, Can. J. Chem. 65(1987)734–739.
[4] J.R. Dias, J. Chem. Educ. 64(1987)213–216; 66(1989), in press.
[5] J.R. Dias, in: *Applications of Discrete Mathematics*, ed. R. Ringeisen and F.S. Roberts (SIAM, Philadelphia, 1988), pp. 148–162.
[6] J.R. Dias, in: *Graph Theory and Topology in Chemistry*, ed. R.B. King and D.H. Rouvray (Elsevier, Amsterdam, 1988), pp. 466–475.
[7] J.R. Dias, *Handbook of Polycyclic Hydrocarbons*, Parts A and B (Elsevier, Amsterdam, 1987 and 1988).
[8] J.R. Dias, MATCH 22(1987)257–268.
[9] D.M.P. Mingos, J. Chem. Soc., Dalton Trans. (1977) 20–25, 26–30, 31–37.
[10] W.C. Herndon, J. Amer. Chem. Soc. 102(1980)1538–1541.
[11] M. Randić and H.E. Zimmerman, Int. J. Quant. Chem.: Quant. Chem. Symp. 20(1986)185–201.
[12] M.B. Hall, I.H. Hillier, J.A. Connor, M.F. Guest and D.R. Lloyd, Mol. Phys. 20(1975)185–201.
[13] M. Elian and R. Hoffmann, Inorg. Chem. 14(1975)1058–1076.
[14] R.B. King, Theor. Chim. Acta 44(1977)223–243.
[15] W.C. Herndon, Tetrahedron 29(1973)3–12.
[16] M. Randić, J. Chem. Soc. Faraday Trans. 2, 72(1976)232–243.
[17] J.R. Dias, J. Mol. Struct. (THEOCHEM), submitted.
[18] T. Živković, N. Trinajstić and M. Randić, Croat. Chem. Acta 49(1977)89;
S.S. D'Amato, B.M. Gimarc and N. Trinajstić, Croat. Chem. Acta 54(1981)1–52;
W.C. Herndon and M.L. Ellzey, Tetrahedron 31(1975)99–107.
[19] G.G. Hall, Trans. Faraday Soc. 53(1957)573; Mol. Phys. 33(1977)551; Bull. Inst. Math. Appl. 17(1981)70.
[20] R.A. Davidson, Theor. Chim. Acta 58(1981)193–231.
[21] References can be found in the following reviews:
(a) E.A. Koerner von Gustorf, F.W. Grevels and I. Fischler (eds.), *The Organic Chemistry of Iron*, Vols. 1 and 2 (Academic Press, San Francisco, 1978, 1981).
(b) F.R. Hartley and S. Patai (eds.), *The Chemistry of the Metal–Carbon Bond*, Vol. 1 (Wiley, New York, 1982).
[22] B.J. Nicholson, J. Amer. Chem. Soc. 88(1966)5156–5165.